Catalysis Communications 69 (2015) 97–103

Contents lists available at ScienceDirect

Catalysis Communications

journal homepage: www.elsevier.com/locate/catcom

Short communication

Palladium nanoparticles supported on reduced graphene oxide as an efficient catalyst for the reduction of benzyl alcohol compounds

Maryam Mirza-Aghayan [a,*], Mahdieh Molaee Tavana [a], Rabah Boukherroub [b]

[a] Chemistry and Chemical Engineering Research Center of Iran (CCERCI), P.O. Box 14335-186, Tehran, Iran
[b] Institut d'Electronique, de Microélectronique et de Nanotechnologie (IEMN, UMR 8520), Cité Scientifique, Avenue Poincaré - CS 60069, 59652 Villeneuve d'Ascq, France

ARTICLE INFO

Article history:
Received 9 February 2015
Received in revised form 9 May 2015
Accepted 28 May 2015
Available online 1 June 2015

Keywords:
Palladium nanoparticles
Reduced graphene oxide
Sonochemical
Benzyl alcohols
Hydrogenolysis
Triethylsilane

ABSTRACT

Palladium nanoparticles were prepared on reduced graphene oxide (Pd NPs/rGO) by using a sonochemical procedure. Pd NPs with a mean diameter of 37 ± 22 nm were deposited on reduced graphene oxide sheets by the reaction between $PdCl_4^{2-}$ and graphene oxide (GO) under sonochemical conditions. The catalyst was characterized by X-ray diffraction (XRD), thermogravimetric analysis (TGA), scanning electron microscopy (SEM), infrared spectroscopy (FT-IR), transmission electron microscopy (TEM) and inductively coupled plasma optical emission spectroscopy (ICP-OES). The Pd NPs/rGO nanocomposite was successfully applied as a reusable catalyst for the reduction of benzyl alcohol derivatives into the corresponding methylene compounds in the presence of triethylsilane. The reductive dehydroxylation of benzyl alcohols takes place under mild conditions affording high yields of the corresponding methylene compounds in short reaction times.

1. Introduction

The transformation of a hydroxyl functional group into the corresponding alkyl group is a delicate process. Alcohol deoxygenation constitutes a powerful synthetic tool especially used in complex natural product synthesis. The Barton–McCombie methodology is the most commonly used, mainly for secondary alcohols, due to its versatility and compatibility with different functional groups [1,2]. The main disadvantage of this reaction is the use of tributylstannane which is toxic, expensive and difficult to remove from the reaction mixture. Since hydroxyl group is a poor leaving group, its transformation into a good leaving group is generally employed [3]. Several reagents and catalysts have been reported for the reduction of benzyl alcohols [4–6]. For example, Pd/C and H_2 in compressed CO_2/water [4], iridium catalyst with hydrazine at 160 °C [5], palladium chloride ($PdCl_2$) and polymethylhydrosiloxane (PMHS) as hydride source [6] have been investigated for this chemical transformation. However, it should be noted that high pressure autoclave or high temperatures and long reaction times were required for this process. Different benzylic alcohols were successfully reduced into the corresponding deoxygenated compounds by using 2.0 equiv. of Ti(III) and 1.5 equiv. of reducing agent such as Mn dust in tetrahydrofuran as solvent [7]. Recently, direct electrolysis of primary alcohols in excess of methyl toluate was reported for the synthesis of the corresponding deoxygenated products in high yield [8].

Organosilanes are used to reduce alcohols to alkanes in the presence of strong Lewis and Brønsted acids [9]. Egi et al. have reported on the direct catalytic deoxygenation of propargyl alcohols with the combination of $H_3[PW_{12}O_{40}]\cdot nH_2O$ (1 mol%) and Et_3SiH in $Cl(CH_2)_2Cl$ or CF_3CH_2OH as solvent [10]. Chan et al. demonstrated the efficiency of $FeCl_3$ as catalyst for the selective dehydroxylation of secondary benzylic alcohols using PMHS as hydride source [11].

We have investigated the efficiency of $Et_3SiH/PdCl_2$ system for several transformations [12–14] such as reduction of benzyl alcohols to the corresponding methylene compounds under homogeneous conditions [15].

Graphene oxide and graphite oxide have been successfully applied as effective heterogeneous catalysts for several organic transformations [16–21].

Noble metal nanoparticles have widely been used as catalysts to promote various chemical reactions [22,23]. Graphite oxide, graphene oxide (GO), reduced graphene oxide (rGO), and graphene in combination with metal nanoparticles have been utilized as catalyst supports [24,25].

In continuation of our efforts on the use of $PdCl_2/Et_3SiH$ system [12–15] and graphite oxide [18–21], we propose in the present study a simple procedure for the preparation of palladium nanoparticles supported reduced graphene oxide (Pd NPs/rGO) under ultrasound conditions (Scheme 1a). The nanocomposite material was characterized using XRD, TGA, SEM, FT-IR, TEM and ICP-OES. The catalytic activity of the Pd NPs/rGO was further investigated for the reduction of benzyl alcohol derivatives into the corresponding methylene compounds in the presence of triethylsilane (Scheme 1b).

* Corresponding author.
E-mail address: m.mirzaaghayan@ccerci.ac.ir (M. Mirza-Aghayan).

http://dx.doi.org/10.1016/j.catcom.2015.05.023
1566-7367/

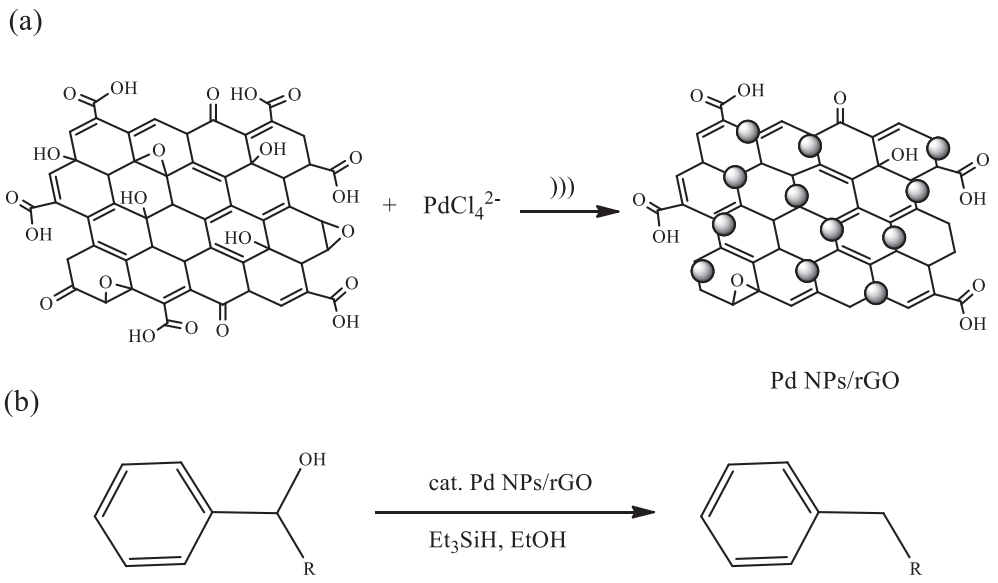

Scheme 1. (a) Synthesis of Pd NPs/rGO using ultrasonication; (b) reduction of benzyl alcohol compounds using Et_3SiH and Pd NPs/rGO nanocomposite catalyst.

2. Experimental

2.1. General information

Elmasonic P ultrasonic cleaning unit (bath ultrasonic) and ultrasonic homogenizer Bandelin Sonoplus HD 3100 (probe ultrasonic) were used to prepare the Pd NPs/rGO nanocomposite samples. X-ray diffraction (XRD) data were collected using a Bruker D8 Advance Theta–2theta diffractometer. Thermogravimetric analysis (TGA) was performed on a NETZSCH TG 209 F1 analyzer. Scanning electron microscopy (SEM) and energy dispersive X-ray (EDX) data were acquired using a VEGA3 LMU TESCAN SEM. IR spectra were recorded from KBr disks with a Bruker Vector 22 FT-IR spectrometer. Transmission electron microscopy (TEM) images were obtained using a Zeiss em900 transmission electron microscope. Palladium content of the Pd NPs/rGO catalyst was determined using ICP-OES Varian 735 ES configuration torch redial instrument after each catalyst sample was completely dissolved in the mixture of HNO_3/HCl (1/3 ratio).

2.2. Synthesis of graphite oxide

Graphite oxide utilized in this work was synthesized according to a previously reported procedure [20].

2.3. Synthesis of palladium nanoparticles/reduced graphene oxide (Pd NPs/rGO)

Typically, 200 mg of graphite oxide powder in 800 mL of deionized water was mixed in a reaction container using bath ultrasonic with a frequency of 37 kHz for 2 h. Then 2 mL of the graphite oxide dispersion

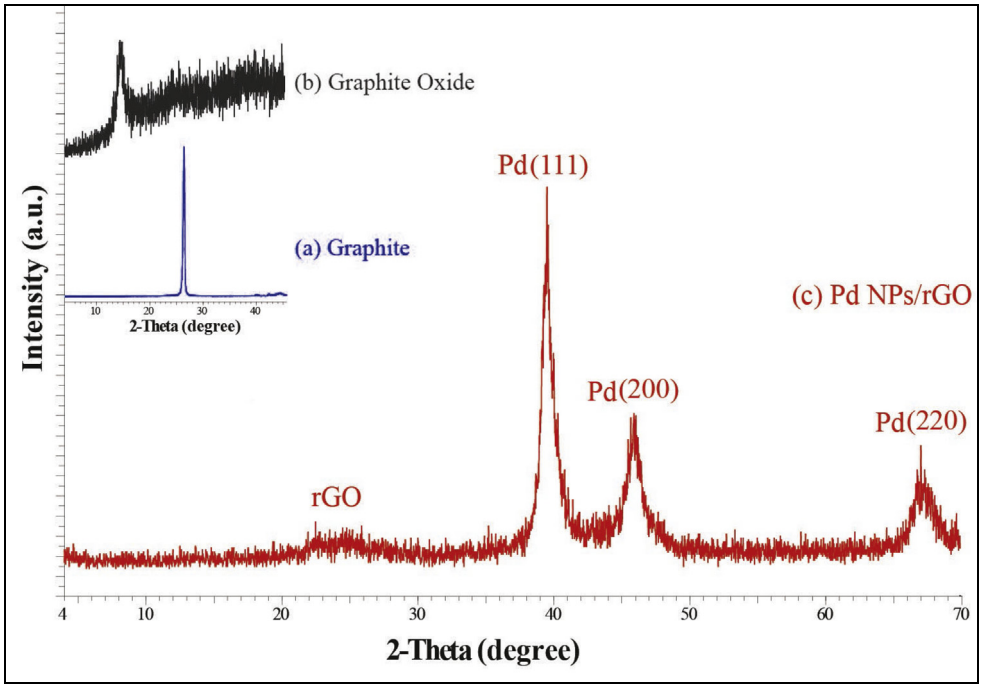

Fig. 1. XRD patterns of (a) graphite, (b) graphite oxide, and (c) Pd NPs/rGO.

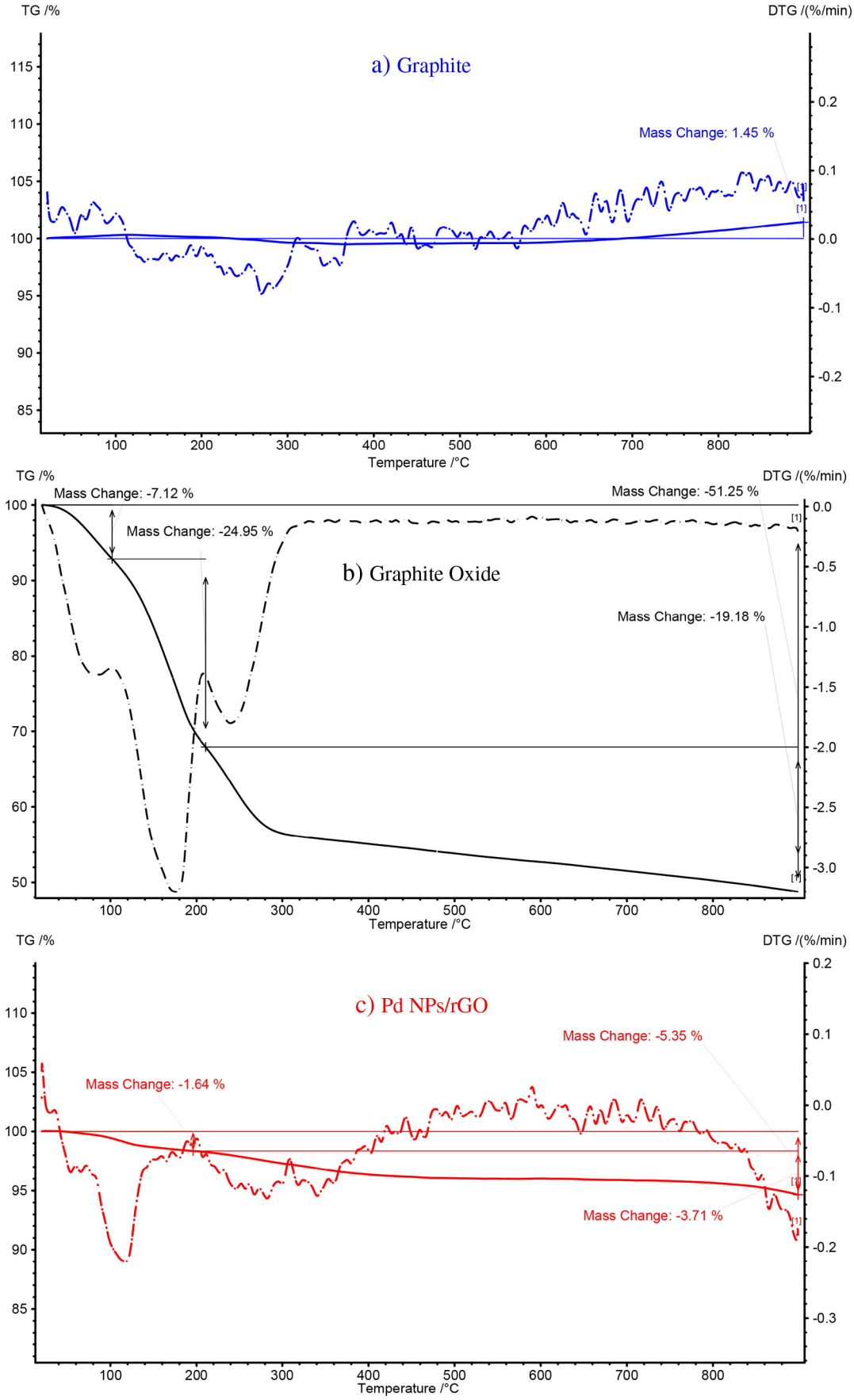

Fig. 2. TGA analysis of (a) graphite, (b) graphite oxide, and (c) Pd NPs/rGO.

with 8 mL of deionized water were mixed for 20 min using bath ultrasonic with a frequency of 80 kHz. Next 0.1 mL of aqueous solution of H_2PdCl_4 (50 mM), prepared by completely dissolving 177.3 mg of $PdCl_2$ in 100 mL of 20 mM HCl solution, was added into the container and mixed for 40 min using probe ultrasonic.

2.4. General procedure for benzyl alcohol hydrogenolysis

To a solution of benzyl alcohol (1 mmol) and triethylsilane (amount indicated in Table 2) in ethanol (5 mL) was added 10 mg of Pd NPs/rGO under an argon atmosphere. The resulting mixture was stirred for the time indicated in Table 2 prior to GC–MS analysis. The resulting mixture was filtered and washed by ethyl acetate for catalyst separation. The pure product in entry 1 was isolated by distillation; for entries 2–10 the products were isolated by column chromatography using hexane/ethyl acetate (9/1) as eluent.

3. Results and discussion

3.1. Preparation and characterization of Pd NPs/rGO nanocomposite

The morphology and chemical composition of the Pd NPs/rGO were characterized by XRD, TGA, SEM, TEM and ICP-OES. Fig. 1 displays typical XRD patterns of the starting graphite, graphite oxide and Pd NPs/rGO nanocomposite. Graphite displays a single and sharp peak at $2\theta = 26.4°$ (Fig. 1a). The disappearance of the graphite peak at $2\theta = 26.4°$ and appearance of a new peak at $2\theta = 11.8°$ confirmed the formation of graphite oxide upon graphite oxidation (Fig. 1b) [20]. The increase of the interlayer spacing value from 3.36 to 4.70 Å for graphite and graphite oxide, respectively, indicates the inclusion of various oxygen containing functional groups and trapped water molecules between the layers during the oxidation process. As shown in Fig. 1c, the XRD pattern of Pd NPs/rGO exhibits characteristic peaks at $2\theta = 39.5°$, 45.9°, 67.4° which can be assigned to the (111), (200), and (220) crystalline planes of the face centered cubic structure of palladium, respectively [26]. A broad peak of very low intensity at about $2\theta = 26°$ indicates the presence of few-layered reduced graphene oxide (rGO) [27]. This result suggests graphite oxide reduction to rGO by partial removal of oxygenated functional groups. The absence of characteristic diffraction peaks of PdO at $2\theta = 33.9°$, 41.9° and 54.8° is in accordance with the reduction of Pd(II) to Pd(0) in this process [28]. The results are in agreement with recent reports on the direct and simultaneous reduction of metal ions and GO using a sonochemical method for the preparation of Au NPs/rGO [29] and Ag NPs/rGO [30] nanocomposites.

TGA confirms the simultaneous conversion of graphite oxide to rGO nanosheets under ultrasonication with the deposition of Pd NPs. Fig. 2

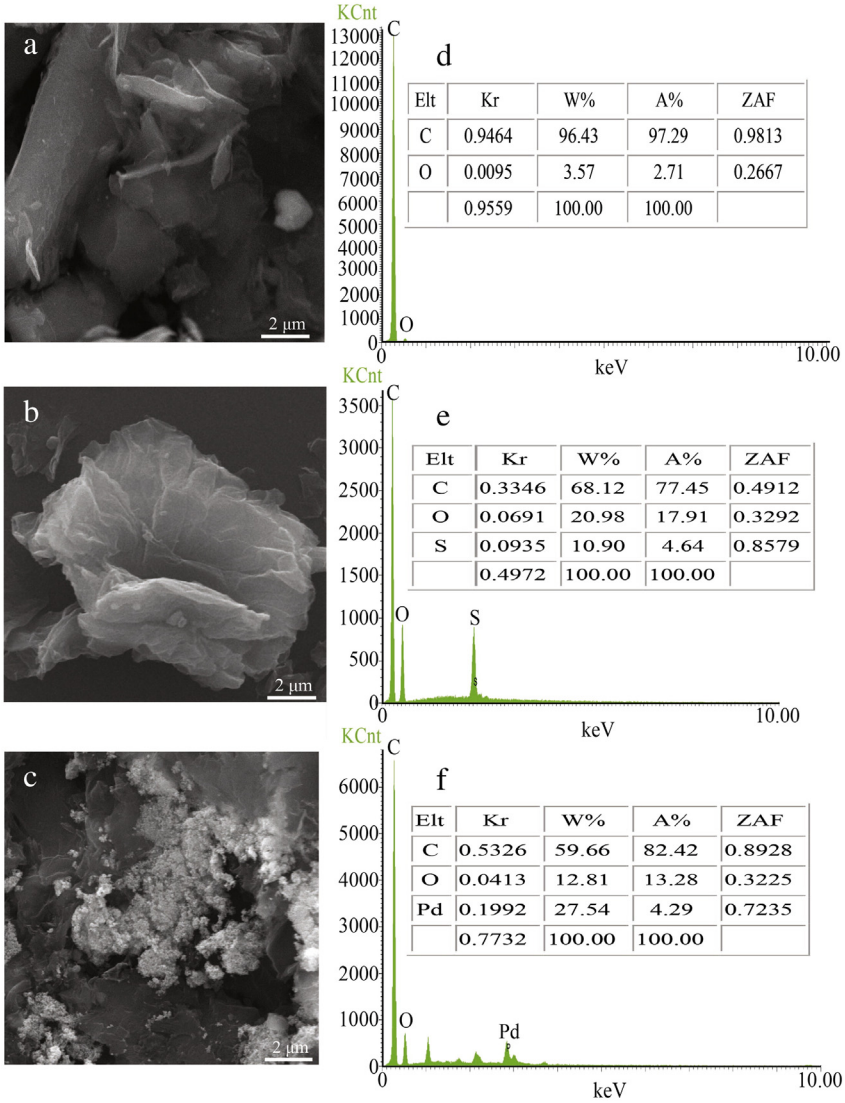

Fig. 3. SEM images of (a) graphite, (b) graphite oxide, (c) Pd NPs/rGO and their respective EDX spectra.

displays the TGA curves of graphite, graphite oxide, and Pd NPs/rGO nanocomposite samples. Graphite material shows a weight loss of nearly 1% in the experimental temperature range (Fig. 2a) [31]. In contrast, the weight loss of graphite oxide occurs in three successive steps. The first one is a steady weight loss (7%), attributed to the vaporization of adsorbed water molecules and occurs at around 100 °C. It is followed by a rapid loss (25%) due to the decomposition of the labile oxygen-containing functional groups (hydroxyl, epoxy, carbonyl, and carboxyl groups) in the temperature range of 100–208 °C. Finally, a weight loss (19%) due to the combustion of the carbon skeleton is observed in the temperature range of 208–900 °C (Fig. 2b) [32]. Pd NPs/rGO exhibited overall less than 10% weight loss in the same temperature range (Fig. 2c). This result indicates the effective reduction of graphite oxide to rGO by removing most of the carboxyl, epoxy, carbonyl, and hydroxyl groups.

Fig. 3 depicts the SEM images and the corresponding EDX spectra of graphite flakes, graphite oxide and Pd NPs/rGO nanocomposite.

As clearly seen in the SEM images, the structure of graphite (Fig. 3a) was completely changed to flower-like structure with appearance of graphitic sheets after the oxidation process (Fig. 3b). EDX analysis shows that the initial graphite comprises mainly carbon (97.29 at.%) with a small amount of oxygen (Fig. 3d). After extensive oxidation of graphite to graphite oxide, EDX spectrum reveals the formation of a new structure with higher oxygen content of 17.91 at.% with C/O ratio of 3.24 (Fig. 3e). It should be noted that the presence of sulfur (4.64 at.%) is most likely due to impurities from H_2SO_4 used in this procedure. The SEM image of the Pd NPs/rGO nanocomposite exhibits a high density of nanoparticles in form of aggregates (Fig. 3c). EDX analysis of Pd NPs/rGO nanocomposite indicates that the palladium loading on the rGO is about 4.29 at.% (Fig. 3f). The FTIR spectrum of graphite oxide exhibits an intensive broad peak of O—H stretching vibrations at about 3393 cm^{-1}, and several bands at 1719, 1574, 1215 and 1044 cm^{-1} assigned to C═O, C═C, (C—O) epoxy and (C—O) alkoxy groups, respectively (Fig. 4a) [33]. The comparison of FT-IR spectra of graphite oxide and Pd NPs/rGO clearly shows that chemical changes occurred during Pd NPs deposition using ultrasonication. The strong peaks at 1719 and 1044 cm^{-1} disappear and a weak peak at 1217 cm^{-1} still remains in the FTIR spectrum of Pd NPs/rGO. The FTIR spectrum is dominated by a broad band at ~1636 cm^{-1} due to C═C stretching modes, suggesting partial restoration of the aromatic network during the chemical process (Fig. 4b) [33].

TEM analysis of the synthesized Pd NPs/rGO material clearly reveals highly exfoliated rGO sheets covered by Pd nanoparticles of 37 ± 22 nm

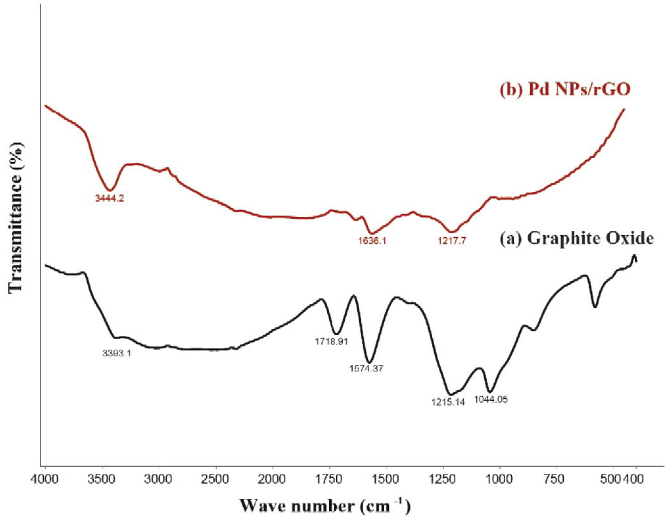

Fig. 4. FT-IR spectra of (a) graphite oxide and (b) Pd NPs/rGO.

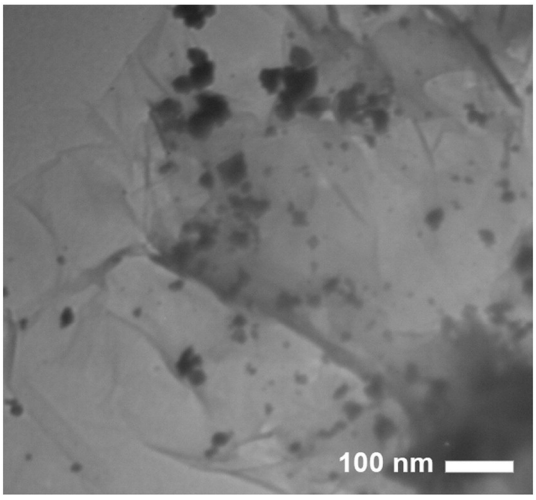

Fig. 5. TEM image of Pd-NP/rGO.

average diameter (Fig. 5). The TEM image of the Pd NPs/rGO also shows nanoparticles in form of aggregates.

3.2. Catalytic performances of Pd NPs/rGO

In connection with our interest in heterogeneous catalysis, we have investigated rGO as a supporting matrix for Pd NPs and Et_3SiH as a hydride source in the chemoselective reductive dehydroxylation of benzylic alcohols. In a control experiment, we have studied the efficiency of graphite oxide (50 mg) for the hydrogenolysis of benzyl alcohol (1 mmol) in ethanol (5 mL). The resulting mixture was stirred for the time indicated in Table 1 prior to GC–MS analysis. Only the starting material was recovered after 5 h (entry 1, Table 1), suggesting that graphite oxide alone is not active for this chemical transformation. In another control experiment, we have tested the efficacy of triethylsilane (2 mmol) for the reductive dehydroxylation of benzyl alcohol in anhydrous ethanol in an inert atmosphere. Again Et_3SiH alone was not effective for the reduction of benzyl alcohol and toluene was obtained only in 8% yield after 5 h (entry 2, Table 1). Finally, we have investigated graphite oxide and Et_3SiH system for this chemical process. After 5 h (entry 3, Table 1), only the starting material was recovered. From this set of control experiments, it is clear that graphite oxide, Et_3SiH or graphite oxide/Et_3SiH is not effective for the reductive dehydroxylation of benzyl alcohol.

In contrast when the reaction of benzyl alcohol (1 mmol) and Et_3SiH (2 mmol) in dry ethanol was performed in the presence of Pd NPs/rGO (50 mg), an exothermic reaction occurred during the first 5 min. GC/MS analysis of the crude product indicated that toluene was obtained in 99% yield after 5 min (entry 4, Table 1). It should be noted that similar results were obtained using only 10 mg of Pd NPs/rGO under otherwise identical experimental conditions (entry 5, Table 1). Decreasing the catalyst amount to 1 mg led to a decrease of the reaction yield to 65% even

Table 1
Different conditions for the hydrogenolysis of benzyl alcohol.

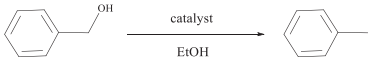

Entry	Catalyst	(mg)	Et_3SiH (mmol)	Time (min)	Yield[a] (%)
1	Graphite oxide	50	–	300	–
2	–		2	150	8
3	Graphite oxide	50	2	300	–
4	Pd NPs/rGO	50	2	5	99
5	Pd NPs/rGO	10	2	5	99
6	Pd NPs/rGO	1	2	5	65

[a] Determined by GC–MS.

Table 2
Reduction of benzyl alcohol derivatives using Pd NPs/rGO catalyst.

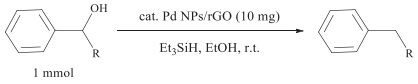

1 mmol

Entry	Substrate	Product	Et_3SiH (mmol)	Time (min)	Yield[a] (%)
1			2	5	99
2			2	15	94
3	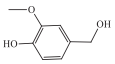		2	10	92
4	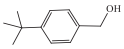	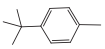	2	10	90
5			2	10	96
6	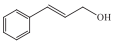		2 4	15 15	47 90
7	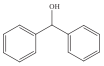		2	20	93
8			2	5	98
9			2 4	30 30	42 82
10			2 4	40 60	35 80
11		–	2 6 6[b]	240 240 240	– – –

[a] Determined by GC–MS.
[b] The reaction was conducted at reflux.

after 1 h. We concluded that 10 mg of Pd NPs/rGO are required for the hydrogenation reaction (entry 6, Table 1).

Under the best reaction conditions, various benzyl alcohols (1 mmol) reacted smoothly with Pd NPs/rGO (10 mg), Et_3SiH (2 mmol) in dry ethanol to give the corresponding methylene compounds at room temperature (Table 2). The reaction of 2-hydroxybenzyl alcohol, 4-hydroxy-3-methoxybenzyl alcohol, 4-*tert*-butyl-benzyl alcohol and 1-phenyl-1-propanol gave the corresponding products in 90–98% yields (entries 1–5, Table 2). We also observed the reduction of conjugated alcohols such as cinnamyl alcohol; propylbenzene was obtained using 2 mmol of Et_3SiH in 47% yield after 15 min at room temperature (entry 6, Table 2). The yield increased to 90% by increasing the amount of Et_3SiH to 4 mmol under the same conditions (entry 6, Table 2). The reaction of benzhydrol and 1-indanol led to the formation of diphenylmethane and indane in 93% and 98% yield, after 20 and 5 min, respectively (entries 7–8, Table 2).

Hydrogenation of 2-furanmethanol and 3-pyridinylmethanol afforded the corresponding 2-methylfuran and 3-methylpyridine in 42 and 35% yield after 30 and 40 min, respectively (entries 9–10, Table 2). Using an excess of triethylsilane (4 mmol) gave 2-methylfuran and 3-methylpyridine in 82 and 80% yield after 30 and 60 min, respectively (entries 9–10, Table 2). Finally, we investigated the reductive dehydroxylation of aliphatic alcohols such as 1-octanol using this procedure. The reduction failed to proceed under these conditions even in the presence of a large excess of Et_3SiH at reflux of solvent (entry 11, Table 2).

It should be noted that this procedure allowed the reduction of benzyl alcohol derivatives in relatively short reaction times and mild conditions as compared to the methods described in the literature [4–6]. For example, benzyl alcohol was reduced in 54% yield after 3 h using Pd/C catalyst in compressed CO_2/water and 1 MPa H_2 [4]. Independently, Huang et al. [5] obtained toluene in 98% yield through the reduction of benzyl alcohol using iridium catalyst with hydrazine at 160 °C after 3 h. Wang et al. [6] reported benzyl alcohol hydrogenolysis in 99% yield using $PdCl_2$ and PMHS after 12 h at 40 °C.

Table 3
Reusability of Pd NPs/rGO catalyst.

Run	1st	2nd	3rd	4th	5th	6th	7th
Yield (%)	99	99	93	92	80	80	79

To evaluate the reusability of the Pd NPs/rGO after completion of the reaction, acetonitrile was added and the mixture was filtered through a sintered funnel to recover the catalyst. The reaction of benzyl alcohol and Et_3SiH in dry ethanol in the presence of 10 mg of the recovered Pd NPs/rGO was performed for seven consecutive cycles. The recycled Pd NPs/rGO was efficient for the hydrogenolysis of benzyl alcohol into the corresponding toluene even after seven consecutive times with an activity loss of about 20% (Table 3). Moreover, to ascertain the leaching of Pd metal, we analyzed the recovered catalyst after seven runs by ICP-OES. The value of Pd in the recovered catalyst was determined to be 0.1 wt.%, which is much lower than 4.38 wt.% determined in the fresh Pd NPs/rGO catalyst. This result indicates that the activity loss of the catalyst after seven consecutive runs was due to Pd leaching.

4. Conclusion

A simple technique was used to synthesize Pd NPs/rGO from graphite oxide and Pd salt in aqueous media using ultrasonic activation. This method does not require any reducing agent. A catalytic amount of Pd NPs/rGO was successfully applied for the hydrogenation of benzyl alcohols to the corresponding methylene derivatives using Et_3SiH in dry ethanol. This new and simple protocol is advantageous as the hydrogenolysis takes place at room temperature, in short reaction times and in high yields, reusable catalyst with a very simple work-up procedure.

References

[1] D.H.R. Barton, S.W. McCombie, A new method for the deoxygenation of secondary alcohols, J. Chem. Soc. Perkin Trans. 1 (16) (1975) 1574–1585.
[2] M.M. Heravi, A. Bakhtiari, Z. Faghihi, Applications of Barton–McCombie reaction in total syntheses, Curr. Org. Synth. 11 (2014) 787–822.
[3] J. Tsuji, In Palladium Reagents and Catalysts: Innovations in Organic Synthesis, 2nd ed. Wiley, Chichester, 2000. 109–168.
[4] H.-W. Lin, C.H. Yen, H. Hsu, C.-S. Tan, CO_2 promoted hydrogenolysis of benzylic compounds in methanol and water, RSC Adv. 3 (2013) 17222–17227.
[5] J.L. Huang, X.J. Dai, C.J. Li, Iridium-catalyzed direct dehydroxylation of alcohols, Eur. J. Org. Chem. 2013 (2013) 6496–6500.
[6] H. Wang, L. Li, X.-F. Bai, J.-Y. Shang, K.-F. Yang, L.-W. Xu, Efficient palladium-catalyzed C—O hydrogenolysis of benzylic alcohols and aromatic ketones with polymethylhydrosiloxane, Adv. Synth. Catal. 355 (2013) 341–347.
[7] H.R. Diéguez, A. López, V. Domingo, J.F. Arteaga, J.A. Dobado, M.M. Herrador, J.F. Quílez del Moral, A.F. Barrero, Weakening C—O bonds: Ti(III), a new reagent for alcohol deoxygenation and carbonyl coupling olefination, J. Am. Chem. Soc. 132 (2009) 254–259.
[8] K. Lam, I.E. Markó, Electrochemical deoxygenation of primary alcohols, Synlett 23 (2012) 1235–1239.
[9] G.L. Larson, J.L. Fry, Ionic and Organometallic-catalyzed Organosilane Reductions, John Wiley & Sons, 2009.
[10] M. Egi, T. Kawai, M. Umemura, S. Akai, Heteropolyacid-catalyzed direct deoxygenation of propargyl and allyl alcohols, J. Org. Chem. 77 (2012) 7092–7097.
[11] L.Y. Chan, J.S.K. Lim, S. Kim, Iron-catalyzed reductive dehydroxylation of benzylic alcohols using polymethylhydrosiloxane (PMHS), Synlett 2011 (2011) 2862–2866.
[12] M. Mirza-Aghayan, R. Boukherroub, M. Bolourtchian, M. Hosseini, Palladium-catalyzed reduction of olefins with triethylsilane, Tetrahedron Lett. 44 (2003) 4579–4580.
[13] M. Mirza-Aghayan, R. Boukherroub, M. Bolourtchian, M. Rahimifard, Palladium catalyzed mild reduction of α, β-unsaturated compounds by triethylsilane, J. Organomet. Chem. 692 (2007) 5113–5116.
[14] M. Mirza-Aghayan, R. Boukherroub, M. Rahimifard, Efficient method for the reduction of carbonyl compounds by triethylsilane catalyzed by $PdCl_2$, J. Organomet. Chem. 693 (2008) 3567–3570.
[15] M. Mirza-Aghayan, R. Boukherroub, M. Rahimifard, A simple and efficient hydrogenation of benzyl alcohols to methylene compounds using triethylsilane and a palladium catalyst, Tetrahedron Lett. 50 (2009) 5930–5932.
[16] M. Spiro, Catalysis by carbons of reactions in solution, Catal. Today 7 (1990) 167–178.
[17] D.R. Dreyer, C.W. Bielawski, Carbocatalysis: heterogeneous carbons finding utility in synthetic chemistry, Chem. Sci. 2 (2011) 1233–1240.
[18] M. Mirza-Aghayan, R. Boukherroub, M. Nemati, M. Rahimifard, Graphite oxide mediated oxidative aromatization of 1,4-dihydropyridines into pyridine derivatives, Tetrahedron Lett. 53 (2012) 2473–2475.
[19] M. Mirza-Aghayan, M. Molaee Tavana, R. Boukherroub, Oxone/iron(II) sulfate/graphite oxide as a highly effective system for oxidation of alcohols under ultrasonic irradiation, Tetrahedron Lett. 55 (2014) 342–345.
[20] M. Mirza-Aghayan, E. Kashef-Azar, R. Boukherroub, Graphite oxide: an efficient reagent for oxidation of alcohols under sonication, Tetrahedron Lett. 53 (2012) 4962–4965.
[21] M. Mirza-Aghayan, S. Zonoubi, M. Molaee Tavana, R. Boukherroub, Ultrasound assisted direct oxidative esterification of aldehydes and alcohols using graphite oxide and oxone, Ultrason. Sonochem. 22 (2015) 359–364.
[22] B. Wu, Y. Kuang, X. Zhang, J. Chen, Noble metal nanoparticles/carbon nanotubes nanohybrids: synthesis and applications, Nano Today 6 (2011) 75–90.
[23] C. Burda, X. Chen, R. Narayanan, M.A. El-Sayed, Chemistry and properties of nanocrystals of different shapes, Chem. Rev. 105 (2005) 1025–1102.
[24] C. Basavaraja, W.J. Kim, Y.D. Kim, D.S. Huh, Synthesis of polyaniline-gold/graphene oxide composite and microwave absorption characteristics of the composite films, Mater. Lett. 65 (2011) 3120–3123.
[25] A.H. Qusti, R.M. Mohamed, M. Abdel Salam, Photocatalytic synthesis of aniline from nitrobenzene using Ag-reduced graphene oxide nanocomposite, Ceram. Int. 40 (2014) 5539–5546.
[26] J. Yang, C. Tian, L. Wang, H. Fu, An effective strategy for small-sized and highly-dispersed palladium nanoparticles supported on graphene with excellent performance for formic acid oxidation, J. Mater. Chem. 21 (2011) 3384–3390.
[27] J. Zhou, Y. Wang, X. Guo, J. Mao, S. Zhang, Etherification of glycerol with isobutene on sulfonated graphene: reaction and separation, Green Chem. 16 (2014) 4669–4679.
[28] Y. Kim, J.G. Kang, S. Lim, J.H. Song, Facile synthesis of monodispersed PdO nanoparticles within mesoporous silica with sonication, Bull. Kor. Chem. Soc. 26 (2005) 1129–1131.
[29] K. Vinodgopal, B. Neppolian, I.V. Lightcap, F. Grieser, M. Ashokkumar, P.V. Kamat, Sonolytic design of graphene–Au nanocomposites. Simultaneous and sequential reduction of graphene oxide and Au(III), J. Phys. Chem. Lett. 1 (2010) 1987–1993.
[30] A. Moradi Golsheikh, N.M. Huang, H.N. Limc, R. Zakaria, One-pot sonochemical synthesis of reduced graphene oxide uniformly decorated with ultrafine silver nanoparticles for non-enzymatic detection of H_2O_2 and optical detection of mercury ions, RSC Adv. 4 (2014) 36401–36411.
[31] S. Santra, P.K. Hota, R. Bhattacharyya, P. Bera, P. Ghosh, S.K. Mandal, Palladium nanoparticles on graphite oxide: a recyclable catalyst for the synthesis of biaryl cores, ACS Catal. 3 (2013) 2776–2789.
[32] Ö. Metin, E. Kayhan, S. Özkar, J.J. Schneider, Palladium nanoparticles supported on chemically derived graphene: an efficient and reusable catalyst for the dehydrogenation of ammonia borane, Int. J. Hydrog. Energy 37 (2012) 8161–8169.
[33] Y. Wang, Y. Zhao, W. He, J. Yin, Y. Su, Palladium nanoparticles supported on reduced graphene oxide: facile synthesis and highly efficient electrocatalytic performance for methanol oxidation, Thin Solid Films 544 (2013) 88–92.